TOWARDS A STATISTICAL THEORY OF TEXTURE EVOLUTION IN POLYCRYSTALS

K. BARMAK*, M. EMELIANENKO†, D. GOLOVATY‡, D. KINDERLEHRER§, AND S. TA'ASAN¶

Abstract. Most technologically useful materials possess polycrystalline microstructures composed of a large number of small monocrystalline grains separated by grain boundaries. The energetics and connectivity of the grain boundary network plays a crucial role in determining the properties of a material across a wide range of scales. A central problem in materials science is to develop technologies capable of producing an arrangement of grains—a texture—that provides for a desired set of material properties.

One of the most challenging aspects of this problem is to understand the role of topological reconfigurations during coarsening. Here we propose an upscaling procedure suitable for large complex systems. The procedure is based on numerical experimentation combined with stochastic tools and consists of large-scale numerical simulations of a system at a microscopic level, statistical analysis of the microscopic data, and formulation of the model based on stochastic characteristics predicted by the statistical analysis. The procedure promises to be valuable in establishing the effective model of microstructural evolution in realistic two- and three-dimensional systems.

To test these ideas we use our upscaling procedure to study the mesoscopic behavior of a reduced one-dimensional network of grain boundaries. Despite the simplicity of its formulation, this model exhibits highly nontrivial behavior characterized by both growth and disappearance of grain boundaries and develops probability distributions similar to those observed in higher-dimensional simulations. Here we focus on the grain deletion events which are common to all coarsening systems.

1. Introduction. Most technologically useful materials arise as polycrystalline microstructures, composed of a myriad of small crystallites, termed grains, separated by interfaces, the grain boundaries. The energetics and connectivity of the boundaries are implicated in many properties across wide scales, for example, functional properties, like electrical conductivity of metal wirings in microprocessors, and lifetime properties, like fracture toughness in structures.

Coarsening consists of the growth and rearrangement of the crystallites, a process which may be interpreted as the anisotropic evolution of a large metastable network. Its control and understanding is a central problem in materials science, the problem of microstructure. It has, after all, been of recognized importance since the stone age (see [15]). Evolution of individual interfaces is governed by known local thermodynamical principles. In addition, facet interchange and grain deletion, coarsening induced variations in topology, introduce network level changes in the system which are stochastic in nature.

In simulation, we are presented with solution trajectories of many thousands of coupled nonlinear partial differential equations representing details of the evolution. Assorted statistics may be harvested and offered up as material properties. But we lack a theory to predict or to verify the presence of stationary, or even stable, fea-

* Department of Materials Science and Engineering, Carnegie Mellon University, Pittsburgh, PA 15213 email: katayun@andrew.cmu.edu.

†Department of Mathematical Sciences, George Mason University, Fairfax, VA 22030 email: memelian@gmu.edu.

‡ Department of Theoretical and Applied Mathematics, The University of Akron, Akron, OH 44325, email: dmitry@math.uakron.edu.

§ Department of Mathematical Sciences, Carnegie Mellon University, Pittsburgh, PA 15213, email: davidk@cmu.edu.

¶ Department of Mathematical Sciences, Carnegie Mellon University, Pittsburgh, PA 15213, email: shlomo@andrew.cmu.edu.

tures of the system. In general, a metastable multiscale process where "upscaling" or "coarse graining" is required for interpretation and subsequent predictive capability, is found increasingly both in engineering and biological applications and represents an interesting direction for computational science. The application of this approach to coarsening in materials, both from simulation and experimental points of view, relies on recently developed computational methods and is new for the study of microstructure. It likewise presents many challenges for mathematical modeling, simulation, and analysis. Obviously, the simulation environment is very flexible and offers us the possibility of interplay with the laboratory.

Historical emphasis in this field has been on the geometry, or more exactly, on statistics of simple geometric features of experimental and simulated polycrystalline networks. Some geometric features of the configuration, like relative area statistics in two-dimensional sections, appear to be properties in the sense that they are robust; however, they are not strongly related to energetics and are, perhaps, better employed as diagnostics. We direct our attention to texture, the mesoscopic description of arrangement and properties of the network described in terms of both geometry and crystallography. It is known that optimizing texture in specific ways improves function, as we observed at the outset. But are there any texture related distributions which are material properties? Recent work has provided us with a new statistic, the grain boundary character distribution, the GBCD, which has enormous promise in this direction. The GBCD is a measure of the relative amount of grain boundary with a given net misorientation. Owing to our new ability to simulate the evolution of large scale systems, we have been able to show that this statistic is robust and, in elementary cases, easily correlated to the grain boundary energy [12],[11], [13].

Our objective is to understand the random processes associated with evolution of polycrystalline networks and the relationship between these processes and GBCD. The first manifestation of random behavior is the grain disappearance event, and so we shall pursue this. For the sake of clarity, our attention within this paper is mostly restricted to the times of these disappearance events, however, the modeling techniques we propose are far more general, as will be demonstrated in subsequent publications.

Our strategy is to conduct numerical experiments with a large computational model valid at the level of microstructure and to obtain the statistical characteristics of the microscopic model through numerical simulations. We target a specific random event (times of disappearance of grains), analyze its statistical properties and derive the appropriate evolution equation that we subsequently solve numerically. Finally we verify that the predictions of both mesoscopic and microscopic models for the rates of grain disappearance events coincide. Although, in this paper we use probabilistic derivation of evolution equations, statistical data can also be interpreted using a Boltzmann-like description [4].

Throughout the presentation, the implementation of our ideas is presented for a simplified model for texture development targeted to capture the stochastic features of network evolution. A simplified, dimensionally reduced model is obtained by removing curvature-driven kinetics of boundary evolution. The model lacks the full physical complexity of a grain growth system due to space reduction, but offers a much more feasible object for mathematical modeling, simulation and analysis. Its physical validity comes from the fact that it retains important statistical properties of network coarsening, specifically, a "relative area histogram" and a "GBCD". More interestingly, identification of the set of stable statistics revealed a close match with the

statistics produced by two-dimensional simulations known from previous literature [9], [11], [13], [22].

The applicability of the evolution equation for disappearance events will subsequently be compared to that obtained for the higher-dimensional grain-growth models. Note that, in the one-dimensional model, the dynamics is essentially governed by the disappearance events, while it raises to a higher level of difficulty in higher-dimensional cases. Understanding the disappearance events for the one-dimensional evolution, can be instrumental to understanding the same events in two and/or three dimensions. Currently we are at the stage of final testing of the numerical models of two- and three-dimensional growth; the techniques developed here will be applied to the results of higher-dimensional simulations as these results become available.

This paper is organized as follows. We start by providing a short account on recent developments in the area that prompted the current study in Section 2. In Section 3, we present a simplified model targeted to capture the stochastic features of network evolution. In Section 3.2, we discuss the results of the large-scale simulations of the simplified model, identify the set of stable statistics and demonstrate the nondiffusive nature of the underlying kinetics. Further, in Section 3.3, we determine the statistical properties of the disappearance events. We show that the waiting times between successive disappearances are independent random variables and find their probability distribution functions (we use the term "waiting time" in agreement with stochastic analysis terminology). The waiting times are *not* identically distributed but rather are time-dependent scalings of an exponential distribution; this reflects the fact that the coarsening process slows down with time.

In Section 4 we develop a generalized master equation for the disappearance events. The master equation can be explicitly solved for the model system and we have found that disappearance rates obtained both analytically and via the numerical experiment are in close agreement with one another (Section 4.2). The form of the probability distribution functions for waiting times suggests that the disappearance events can be approximated as a stationary Poisson process at the initial stages of evolution and by a continuous time random walk (CTRW) at the later stages, respectively. This conjecture has also been verified by comparing the theoretical predictions to the numerical experiment. In Section 5 we review the traditional CTRW theory, which offers a simpler way to handle the complexity of the intermediate stages of the jump process. We further compare the statistics obtained by direct simulation with the solution of the fractional diffusion equation developed through CTRW theory.

Suggested above is that there are several regimes exhibited by grain disappearance waiting time distribution that have an affect on the evolution of the grain boundary character distribution evolution. We are obliged to consider all of them, the rapid relaxation, the middle regime, and the end regime not only for thoroughness but also because it is unknown which regimes will be observed in practice.

2. Disappearance events: background and motivation. We begin with a short perspective. The regular evolution of a network of grain boundaries in two dimensions, sometimes referred to as normal grain growth, [3], is governed by the Mullins equation of curvature driven growth supplemented by the Herring condition of force balance at triple junctions—a system of parabolic equations with coercive boundary conditions, [1], [5], [14], [17]. (For the higher dimensional case, see [12].) When applied to an individual grain in an ensemble whose grain boundary energy is constant, this mechanism leads to the von Neumann-Mullins $n-6$ rule [16]: the rate

of change of the area of an n-sided grain is proportional to $n-6$, i.e.,

$$\frac{dA_n}{dt} = c(n-6), \text{ where } A_n \text{ is the area of an } n-\text{sided grain}, \tag{2.1}$$

and $c > 0$ is a material constant. Inspection of Fig.2.1 shows that, contrary to (2.1), the average area of five-sided grains in a columnar aluminum structure increases several-fold during coarsening. This does not imply that (2.1) fails, but rather that most of the grains observed at the time $t = 2$ hours, for example, had $6, 7, 8, \ldots$ sides at some earlier time $t < 2$ hours. Thus in the network setting, the topological changes (disappearance events and facet interchanges) play a major role.

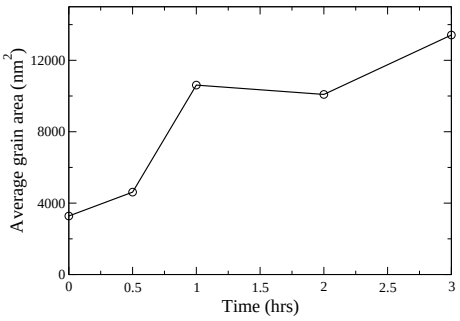

FIG. 2.1. *Average area of five sided grains in an Al columnar structure.*

Although small grains with small numbers of sides will be deleted, their effect on the configuration is essentially random. A significant difficulty in developing a theory of the GBCD lies in the lack of understanding of the relationship between these stochastic events and coarsening. This is the reason why the study of the network aspect of grain boundary system is so important. As a first step, it is natural to consider the following model. Suppose that high energy boundaries are preferentially deleted in favor of lower energy ones, for example, through the motion of triple junctions where a low energy boundary segment is present, and new boundaries are created and disappear at random. This is, in fact, what we observe. A Langevin equation for the misorientation angle α expresses this,

$$d\alpha_t = -\gamma'(\alpha) + \epsilon dB_t, \tag{2.2}$$

where dB_t is white noise. Above, α represents the difference of lattice orientations on either side of the boundary, the lattice misorientation, $\gamma(\alpha)$ represents the energy of the boundary, and ϵ is related to the rate at which new grain boundaries enter the system. The stationary distribution for α is given by the Boltzmann-like expression

$$\rho(\alpha) = \frac{1}{Z} e^{-\frac{2\gamma(\alpha)}{\epsilon^2}},$$

where Z is a normalizing constant, that can be found by solving the stationary Fokker-Planck equation associated to (2.2). This distribution is actually what is found, both in our experiments (Fig. 3.2) and large-scale 2-dimensional simulations [11], [13]. Unfortunately, (2.2) is a naive description of the coarsening process, so we need to study network behavior in greater depth. This is the main focus of the present paper.

3. Reduced model - a simple coarsening network.

3.1. Model description. In this section we define and analyze the properties of the simple coarsening network—a system of grain boundaries represented by intervals on the line. We assume that each grain boundary is described by its length and a prescribed "misorientation". There will be only nearest neighbor interactions

between the boundaries with the strength of the interactions dependent on relative misorientation of the neighboring boundaries.

For a fixed $L > 0$, consider a partition of a circle of circumference L by n randomly chosen points. This is equivalent to partitioning the interval $[0, L] \subset \mathbf{R}$ by the points $x_i, i = 1, \ldots, n$ where $x_i \leq x_{i+1},\ i = 1, \ldots, n-1$ and the point x_{n+1} is identified with the point x_1. Given the periodicity assumption, the interval $[0, L]$ is thus subdivided into n intervals $[x_i, x_{i+1}],\ i = 1, \ldots, n$ of the lengths $x_{i+1} - x_i,\ i = 1, \ldots, n-1$ and $L + x_1 - x_n$, respectively. Note that the locations and the number of points will vary during evolution, however the total length L of all intervals remains fixed. Further, if a partition point leaves $[0, L]$ through $x = 0$, it immediately reenters $[0, L]$ at $x = L$ and vice versa.

For each interval $[x_i, x_{i+1}],\ i = 1, \ldots, n$, we select a random number $\alpha_i \in \mathbf{R}$. The intervals $[x_i, x_{i+1}]$ correspond to grain boundaries and the points x_i represent the triple junctions. The parameters $\{\alpha_i\}_{i=1,\ldots,n}$ can be viewed as representing crystallographic misorientations. The length of the i^{th} grain boundary is given by $l_i = x_{i+1} - x_i$. Now choose a non-negative energy density $f(\alpha)$ and define the energy

$$E(t) = \sum_{i=1}^{n} f(\alpha_i)(x_{i+1}(t) - x_i(t)). \tag{3.1}$$

Consider gradient flow dynamics characterized by the system of ordinary differential equations

$$\dot{x}_i = f(\alpha_{i+1}) - f(\alpha_i),\ i = 2, \ldots, n, \text{ and } \dot{x}_1 = f(\alpha_1) - f(\alpha_n). \tag{3.2}$$

The parameter α_i is prescribed for each grain boundary initially according to some random distribution and does not change during its lifetime. The velocities of the grain boundary i can be computed from the relation

$$v_i = \dot{x}_{i+1} - \dot{x}_i = f(\alpha_{i+1}) + f(\alpha_{i-1}) - 2f(\alpha_i) \tag{3.3}$$

The grain boundary velocities remain constant until the moment when one of the boundaries collapses. The velocity of that boundary is then removed from the list of the current grain velocities and two velocities of its neighbors are changed due to the creation of a new triple junction. Every such disappearance event rearranges the grain boundary network and, therefore, affects its subsequent evolution. Note that the lengths of the individual grain boundaries vary linearly between the disappearance events and depend entirely on the respective grain boundary velocities.

An important feature of the thermodynamics of the normal grain growth is that it is energy dissipative. Our reduced gradient flow model (3.2) is specifically designed to enforce dissipation. To verify this, first consider a time t between any two disappearance events. Then

$$\begin{aligned}
\frac{dE}{dt} &= \sum f(\alpha_i) v_i \\
&= \sum f(\alpha_i)(f(\alpha_{i+1}) - f(\alpha_i) - f(\alpha_i) + f(\alpha_{i-1})) \\
&= \sum f(\alpha_i)(f(\alpha_{i+1}) - f(\alpha_i)) - f(\alpha_i)(f(\alpha_i) - f(\alpha_{i-1})) \\
&= \sum f(\alpha_i)(f(\alpha_{i+1}) - f(\alpha_i)) - f(\alpha_{i+1})(f(\alpha_{i+1}) - f(\alpha_i)) \\
&= -\sum (f(\alpha_{i+1}) - f(\alpha_i))^2
\end{aligned}$$

by periodicity and relabeling of indices. This also follows from the fact that for any gradient flow dynamics

$$(\dot{x}_i)^2 = -\frac{\partial E}{\partial x_i}\dot{x}_i,$$

so that $\frac{\partial E}{\partial t} = -\sum \dot{x}_i^2 < 0$. Now suppose that a grain boundary $[x_c, x_{c+1}]$ vanishes at time $t = t_c$ and it is the only grain boundary vanishing at t_c. Then the velocity of that boundary $v_c(t) < 0,\ t < t_c$, namely,

$$\frac{1}{2}(f(\alpha_{c+1}) + f(\alpha_{c-1})) < f(\alpha_c).$$

and $l_c \to 0$ for $t \to t_c^-$. Now $E(t) > \sum_{i\neq c} f(\alpha_i) l_i,\ t < t_c$, and

$$E(t_c) = \lim_{t\to t_c} \sum_{i\neq c} f(\alpha_i) l_i \leqq \lim_{t\to t_c} E(t).$$

Thus the model system is indeed dissipative.

From the materials science perspective, it is important to know the distributions of relative lengths, the geometric statistics, as well as the total area of grains with certain grain misorientations. In our reduced gradient flow model, the state space is $S := \{(l, v, \alpha)\}$, where $l \in \mathbb{R}^+,\ v \in \mathbb{R},\ \alpha \in (a, b)$. Then the dynamics of the system (3.2) can be described at a mesoscopic level by solving the set of evolution equations for the joint probability density function $\rho(l, v, \alpha, t)$. A somewhat easier task is to understand the dynamics of the disappearance events—the rates at which these events are likely to occur as well as the distributions of accompanying velocity changes. The difficulty is that there is no a priory information regarding statistical properties associated with disappearance events; this information has to be harvested from either laboratory or numerical experimentation. We follow the latter route in the next section.

3.2. Simulation results and validation. The first step toward a mesoscopic model is the identification of stable statistics. To this end, we simulated the reduced gradient flow model described in Section 3. For each simulation run, a system of n grain boundaries on the interval $[0, L]$ was considered with the partition points $\{x_i\}_{i=1}^n$ and the misorientation parameters $\{\alpha_i\}_{i=1}^n$ randomly chosen according to a uniform distribution. The resulting collection of segments was subsequently allowed to evolve according to the coupled system of ordinary differential equations (3.2). For each of the segments, the disappearance times were calculated and the minimum of these times was taken across all segments. Then the number of grain boundaries was decreased (with remaining lengths preserved and velocities adjusted to the new configuration) and the simulation was continued. This process was repeated until a stopping criterion was reached. Since the main goal of this procedure was to obtain statistical information, the simulation was stopped when the size of the sample became too small. This simulation was repeated many times by varying the initial grain boundary configuration.

In what follows, we refer to each grain boundary disappearance event as a simulation "step" and to each simulation run as a "trial". Hence, unless there are coincident events, 10^4 boundaries disappear exactly after 10^4 steps. The statistics of several numerical experiments for s system of 10^4 grain boundaries is presented below. The runs are initialized with a random configuration of misorientations and lengths and

use the same energy functional $f(x) = (x - 0.5)^2$, unless noted otherwise. The grain boundary character distribution (GBCD) is computed as $\sum_{i=1}^{n} l_i \delta(\alpha - \alpha_i)$, which measures the total length of grain boundaries with a particular misorientation parameter α_i.

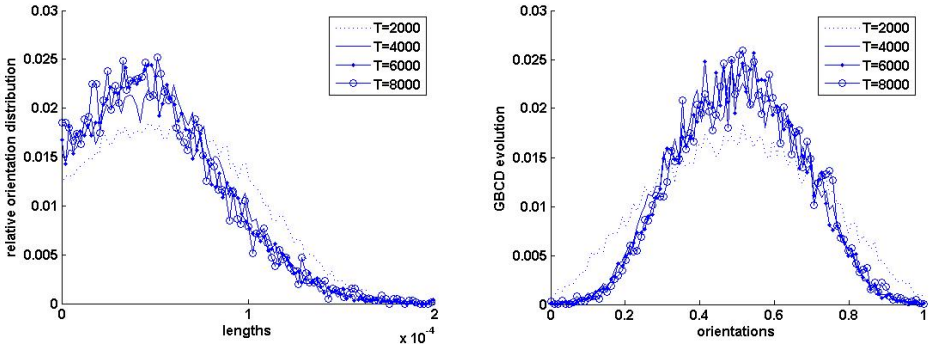

FIG. 3.1. *Evolution of the probability densities of: (a) relative lengths, (b) grain boundary character distribution, i.e. total lengths occupied by particular misorientation, for the choice of* $f = (x - 0.5)^2$. *Both distributions stabilize early in the simulation and remain stable until very last stages.*

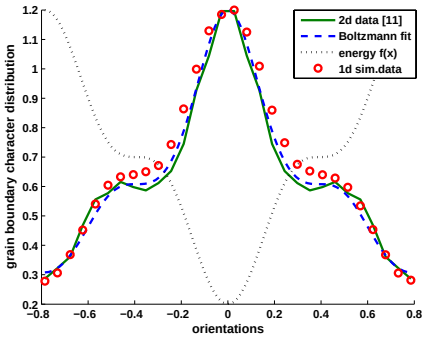

FIG. 3.2. *Comparing GBCD for* $f(x) = 1 + 0.02(1 - (cos(4x))^3)$ *obtained via reduced gradient flow, large-scale two-dimensional simulations, and Boltzmann distribution. Evidence of inverse correlation between grain boundary character distributions and interfacial energies, as well as Boltzmann shape are preserved in the reduced model.*

Figure 3.1 shows evolution of the relative length and grain boundary character distributions for the choice of a quadratic potential. Neither statistic changes its shape in the latter part of the simulation up until a moment when too few grain boundaries remain in the system. To compute the *relative* length distribution, we scale the total number of elements in each bin by the value of the mean length $\langle l \rangle$ at a particular moment during simulation (similar to how relative area distributions are computed in higher-dimensional simulations and experiments [11]). We clearly observe stabilization of both distributions. The existence of stable statistics for both lengths and misorientations is a strong evidence that a well-defined statistical model can be formulated for this type of dynamics.

In Figure 3.2 we compare the reduced-model analog of the GBCD obtained from our computational experiments with the numerical results for the two-dimensional, large-scale simulations ([11]). The graphs clearly show that the shapes of f and the corresponding misorientation distribution are inversely correlated. This is a natural consequence of the fact that the lower energy boundaries dominate those with higher energy. Importantly, GBCD in the reduced system is shown to have a very good match with its two-dimensional counterpart and is in almost perfect agreement with the shape given by a Boltzmann distribution. These observations show that the reduced gradient flow model has the same generic features as the physically realistic three-dimensional model.

Relying on our microscopic reduced model description and statistics harvested from the corresponding deterministic simulation, we want to find a suitable analytical description that would match our numerical observations. To the best of our knowledge, none of the previously conducted investigations into grain growth phenomena succeeded in understanding the role of disappearance events during evolution, hence we cannot rely on any a priori knowledge of such processes. As was mentioned earlier, in this paper we want to gain some computational insight into the system evolution by analyzing the statistical characteristics of the times of disappearance events.

3.3. Computational analysis of waiting times. To understand the statistics associated with evolution of the reduced gradient flow system, a large collection of data was harvested from the microscopic model via direct simulation of the system of ordinary differential equations (3.2). By interrogating this dataset, we want to identify basic characteristics of the main statistical model parameters. In all tests that follow, we use data collected from $1.5 \cdot 10^4$ trial runs each containing $5 \cdot 10^3$ grain boundaries.

First, we want to verify whether the waiting times between disappearance events can be regarded as independent random variables. Let T_1 be the waiting time before the first disappearance event and set T_i to be the waiting time between the $(i-1)$-st and the ith disappearance events for every $i = 2, \ldots, n$. Note that T_i is a random variable for each $i = 1, \ldots, n$ due to the randomness of the initial data.

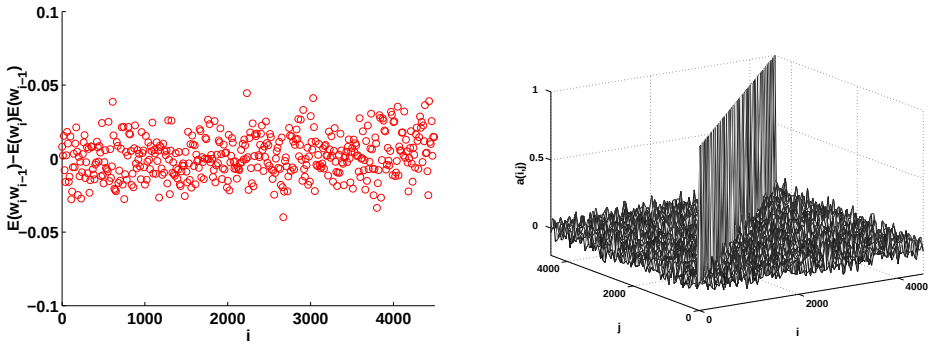

FIG. 3.3. *(a) Correlation between the consecutive waiting times as a function of the index of the disappearance event. (b) Evidence of the diagonal dominance of the correlation matrix. The plot represents the correlation $a(i, j)$ between variables T_i and T_j.*

In Figure 3.3(a) we plot the correlation coefficient between T_i and T_{i-1}, where i ranges from 1 to $4.5 \cdot 10^3$. Observe that the correlation between neighbors does not grow with time. Figure 3.3(b) depicts a typical shape of the correlation matrix

$A = \{a(i,j)\} = \left\{c(i,j)/\sqrt{c(i,i)c(j,j)}\right\}$ between the variables T_i and T_j, with $i, j = 1, \ldots, n$. Here $C = \{c(i,j)\}$ is the corresponding covariance matrix constructed from our $1.5 \cdot 10^4 \times 5 \cdot 10^3$ dataset. The matrix is close to being diagonal, with all off-diagonal entries limited in absolute values by 0.05 and all diagonal entries equal to 1, which suggests that there is no significant correlation between the waiting times.

The next question is to identify the distribution function $w_i(t)$ for the waiting time T_i, $i = 1, \ldots, n$. The answer is provided by Figure 3.4. In the first of the two pictures, we plot the histograms of $w_i(t)$ for every 100-th waiting time, starting with step number 100 and ending with step 4500. Due to a dramatic change of characteristic scale during the course of the simulation, we scale the time axis by dividing time range of each distribution by the corresponding maximum, so that it ranges from 0 to 1, to make all curves visible. The fact that all curves lie on top of each other suggests a common form for the distribution law. The second plot Fig. 3.4(b) shows the behavior of distributions $w_i(t)$ on a log-normal scale given for every 500 steps starting with step number 2000 for visual clarity. It is obvious that all curves have a linear trend on a log-normal scale, showing that each probability density exhibits an exponential behavior. However, as clearly visible in Figure 3.4(b), the means of the exponential distributions increase with time, due to the slowdown of the grain growth dynamics attributed to the decreasing variability of grain boundary misorientations and to the increasing average grain boundary length.

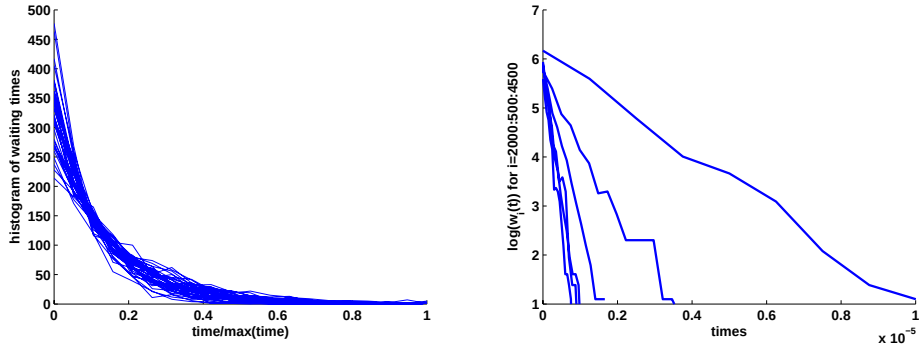

FIG. 3.4. *(a) Histograms of waiting times $w_i(t)$ for $i = 100, 200, \ldots, 4500$ vs. times scaled to range from 0 to 1. (b) Log-normal scale plot of the histograms for waiting times $w_i(t), i = 2000, 2500, \ldots, 4500$, reveals exponential behavior with decaying rates.*

Hence we conclude that the waiting times distributions depend on the step number i and are given by

$$w_i(t) = r_i \exp(-r_i t),$$

where r_i is a constant dependent on i.

Having made these observations, we can use probabilistic arguments to understand how the rates at which the disappearances are observed depend on time and to write down the corresponding evolution equations. Note, however, that non-identically distributed waiting times are beyond the scope of the traditionally used theories, e.g. the theory of random walks or standard renewal processes.

4. Modeling non-homogeneous waiting times. Here we use the statistical properties of the waiting times determined in the previous section to derive the meso-

scopic model for the rate of disappearance events.

4.1. Renewal master equation. Let us consider the sequence of disappearance events during the grain coarsening. These events can be described within the framework of a traditional renewal process theory as long as the waiting times $T_1, T_2, \ldots$ between consecutive events are independent, identically distributed random variables [6, 7, 10]. Here we must deal with a more general case, where $T_i,\ i = 1, 2, \ldots$ are nonnegative, independent random variables that *may not be identically distributed*, that is each T_i is drawn from its own distribution $w_i(t),\ i = 1, 2, \ldots$.

Set $t_0 = 0$ and let

$$t_k = \sum_{i=0}^{k} T_i, k \geq 1 \tag{4.1}$$

be the time of the k-th jump. Consider the random process

$$N(t) = \max\{k \geq 0 : t_k \leq t\} \tag{4.2}$$

counting the number of jumps up to time t. Denote the probability that at least k disappearances have occurred prior to time t by

$$\Lambda_k(t) = \mathtt{P}(t_k \leq t), \tag{4.3}$$

and the corresponding density function by

$$\lambda_k(t) = \frac{d\Lambda_k(t)}{dt}. \tag{4.4}$$

Note that $\lambda_k(t)dt$ is the probability that the k-th disappearance occurs during the time interval $[t, t + dt]$. The probability that some disappearance will be observed during the same time interval is given by

$$\lambda(t)dt = \mathtt{P}\left(\cup_k \{t_k \in [t, t + dt]\}\right) = \sum_{k=1}^{\infty} \lambda_k(t)dt, \tag{4.5}$$

where the last equality follows if we assume that

$$\mathtt{P}\left(\{t_n \in [t, t + dt]\} \cap \{t_{n+1} \in [t, t + dt]\}\right) = 0,$$

for any $n \geq 1$ when dt is small enough. We call $\lambda(t)$ the disappearance rate.

Since the quantity $\Lambda_k(t)$ is a sum of mutually independent random variables $T_i,\ i = 1, \ldots,\ k$, the density $\lambda_k(t)$ can be computed as a k-fold convolution of the waiting time densities $w_i(t),\ i = 1, \ldots,\ k$, so that

$$\lambda_k(t) = \int_0^t \int_0^{t-s_1} \ldots \int_0^{t-s_1-\ldots-s_{k-2}} w_1(s_1)w_2(s_2)\ldots w_{k-1}(t - s_1 - \ldots - s_{k-1})ds_{k-1}\ldots ds_1. \tag{4.6}$$

We can construct the master equation as follows. Observe that

$$\lambda_{k+1}(t) = \int_0^t \lambda_k(s)w_{k+1}(t - s)ds, \tag{4.7}$$

that is, every $(k+1)$-st disappearance event at the time t has its k-th predecessor at some time $s < t$. Then, assuming that we can interchange summation and integration,

$$\begin{aligned}\lambda(t) &= \lambda_1(t) + \textstyle\sum_{k=1}^{\infty} \lambda_{k+1}(t) = w_1(t) + \sum_{k=1}^{\infty} \int_0^t \lambda_k(s) w_{k+1}(t-s) ds \\ &= w_1(t) + \int_0^t \lambda(s) \sum_{k=1}^{\infty} \frac{\lambda_k(s)}{\lambda(s)} w_{k+1}(t-s) ds \\ &= w_1(t) + \int_0^t \lambda(s) W(s, t-s) ds,\end{aligned}$$

where

$$W(s, t-s) := \sum_{k=1}^{\infty} \frac{\lambda_k(s)}{\lambda(s)} w_{k+1}(t-s) \tag{4.8}$$

is the kernel describing the overall probability that a disappearance event at the time s will be followed by another such event $t-s$ units of time later. Note that, by the definition of λ, we can treat the ratio $\lambda_k(t)/\lambda(t)$ as a probability that a disappearance event observed during the time interval $[t, t+dt]$ is the k-th such event from the beginning of the simulation.

We conclude that the disappearance rates satisfy

$$\lambda(t) = w_1(t) + \int_0^t \lambda(s) W(s, t-s) ds, \tag{4.9}$$

which will be referred to as a generalized renewal equation from now on. In the case of the waiting times distributed according to a common law $w_k(t) = w(t)$, $k \geq 1$, we obtain a standard renewal equation (cf. [7])

$$\lambda(t) = w(t) + \int_0^t \lambda(s) w(t-s) ds. \tag{4.10}$$

This equation, in turn, yields $\lambda(t) = r = const$ in the case of a regular Poisson process when $w(t) = re^{-rt}$. Notice, however, that the behavior of the disappearance rate is more complicated in the case of non-identically distributed waiting times. For instance, if $w_i(t) = r_i e^{-r_i t}$, by a simple but tedious calculation of k-fold convolutions we can solve (4.9) to obtain

$$\lambda(t) = \sum_{k=1}^{\infty} \sum_{i=1}^{k} r_i e^{-r_i t} \prod_{j=1, j\neq i}^{k} \frac{r_j}{r_i - r_j}. \tag{4.11}$$

In order to avoid possible convergence issues and to reflect the fact that the number of events in the model systems is finite we will assume that the first summation in (4.11) is performed up to a large $m < \infty$.

We now compare the computational results based on a MATLAB implementation of the expression (4.11) with those obtained via microscopic simulation of our reduced gradient flow system as discussed above.

4.2. Numerical experiments based on renewal theory. First notice that the dependence of r_i on i is quartic, as demonstrated by the least-squares fit in Figure 4.1(a). Hence $r_i \sim (N_\infty - i)^4$, where N_∞ denotes the total number of disappearance events in the simulation. Since the number of disappearance events is equal to the

number of grain boundaries in the system at $t = 0$, here $N_\infty = 4.5 \cdot 10^3$. This gives precise characterization of $w_i(t)$ in the previous analysis.

Combining this result with the analytical solution of the generalized renewal equation (4.11) we see that it predicts the complex behavior observed in our experiments. Indeed, Figure 4.1(b) shows good agreement of the analytical and simulated disappearance rates for a relatively long period within the simulation timespan. The fact that the validity of the derived generalized equation is preserved for so long makes it a very robust estimate for system behavior.

Examining the expression $r_i \sim (N_\infty - i)^4$, we observe that $r_i \approx N_\infty^4$ for $i \ll N_\infty$ hence, at its initial stages, the renewal process is close to a stationary Poisson process.

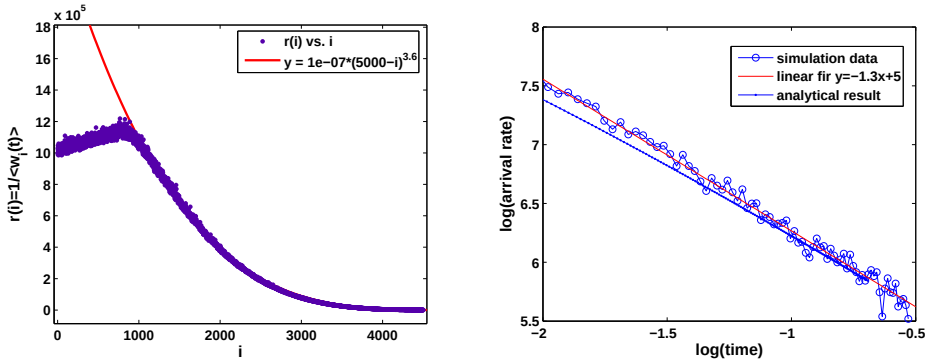

FIG. 4.1. *(a) Least squares fit for the exponential distribution parameters r_i. (b) (circles) empirical disappearance rate at time t produced via simulation in log-log scale, (dashed line) linear least squares fit, (solid line) analytical result obtained via equation (4.11) corresponding to the waiting times $w_i(t) = r_i \exp(-r_i t)$ with $r_i = 3.7e-9(1400-i)^4$ and $i = 3600$ through $i = 4500$.*

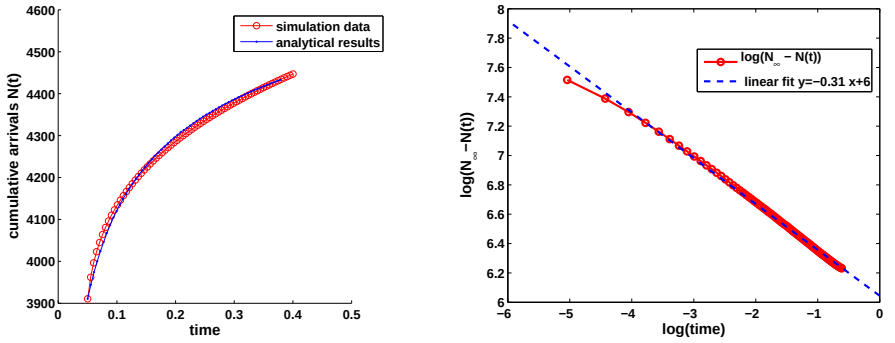

FIG. 4.2. *(a)(circles) Empirical cumulative number of disappearance events at a time t produced by simulation, (solid line) analytical result obtained from the generalized renewal equation (4.9) with $w(t) \sim t^{-1.3}$. (b) (a) Least square power law fit for the number of surviving grain boundaries at time t.*

However, our numerical experiments show that the cumulative disappearances do not behave linearly with respect to time overall.

Figures 4.2(a) and (b) depict $N_\infty - N(t)$, the number of intervals in the system surviving at time t for the period from 1000 to 4500-th disappearances, and the disappearance rate for the same period of time, respectively. This behavior conforms

well with $N(t) \sim t$ in the beginning. However, when we analyze $N_\infty - N(t)$ vs. t with t between 3000th and 5000th disappearances (Figure 4.2(b)), we notice that

$$N_\infty - N(t) \sim t^{-\beta}, \text{ where } \beta \sim 0.3.$$

The dynamics of the process experience a transition from one mode to another at some critical point t_{cr} in the simulation. At the same critical time t_{cr} the stabilization of relative distributions is observed. Note that, although by the time $t = t_{cr}$ almost half of the boundaries have disappeared, the absolute time elapsed from the onset of simulation remains minuscule (of the order of 10^{-2} sec for a 100 sec long simulation). The change in the behavior of the system can be attributed to "washing-out" of transients during the relaxation stage until it reaches the steady state.

The deviation from Poisson behavior is easily captured by the generalized renewal equation derived earlier. However, what is even more intriguing is that the disappearance times match those obtained via the regular renewal equation for the choice of $w(t) = 0.051\, t^{-1.3}$, as shown by the solid line in Figure 4.2(a). Similar correspondence is demonstrated by the plot of the number of surviving grain boundaries at a time t (Figure 4.2(b)). This suggests the existence of an intermediate fractional diffusive regime in our model (see the Appendix) that we will discuss next. As we will show, while the generalized equation (4.11) has the advantage of reproducing all stages of the system evolution, the intermediate stages of evolution admit a reasonably good approximation by means of a more simple set of equations.

5. Modeling intermediate stages of the simulation.

5.1. Continuous time random walk approach—derivation of a master equation. In the standard theory of continuous time random walks, one usually adheres to the following basic description originally due to Montroll and Weiss [23]. Consider a walker making random steps in a state space X. Let the walk be homogeneous in the following sense: if the walker arrives at a point x at a time t, the probability $\phi(y, s)$ of making the next step of size y after a pause s depends on y and s, but not on x and t. Also, assume that the transition probability density ϕ can be factored into a product of a function of time and a function of step length:

$$\phi(y, s) = \mu(y)w(s). \tag{5.1}$$

Here $w(s)$ is the waiting time density and $\mu(y)$ is the step-length density defined as the marginals of the transition density ϕ. This separability assumption of the Montroll-Weiss model [10], [23] will be considered in what follows for the sake of simplicity.

Let $P(x, t)$ be the occupancy probability, i.e. the probability of finding the walker at the state x at time t, given that at time zero the walker was at the origin, i.e. $P(x, 0) = \delta(x)$. Due to the homogeneity assumption above, if the walker arrives at x' at time t', the probability of finding him at x at time t is $P(x - x', t - t')$. Given w, we can compute the probability that a walker arriving at a site pauses for at least time t before leaving that site: $\psi(t) = 1 - \int_0^t w(t')dt'$.

The occupancy density P and the transition probability density $\phi(x, t)$ are related via a master equation that we can formally derive. At time t either the walker has never left the starting site, or he has made at least one step. The probability of the former has the density $\psi(t)$ and the corresponding contribution to $P(x, t)$ is given by $\psi(t)\delta(x)$. If the walker makes one or more jumps, we may partition all possible motions over the outcome and time of occurrence

$$P(x, t) = \delta(x)\psi(t) + \int_0^t \int_{-\infty}^{\infty} P(x - x', t - t')\mu(x')w(t')dx'dt'. \tag{5.2}$$

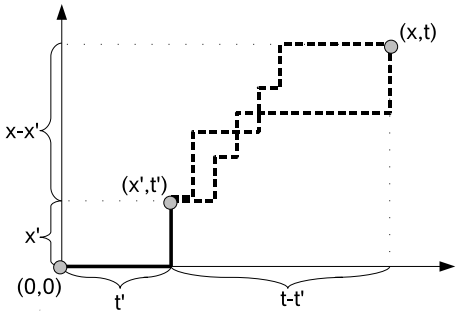

FIG. 5.1. *Random walk: partitioning over the first jump.*

Intuitively, the first term on the right-hand side above accounts for a walker who fails to move from the starting position before time t elapses. The integral expresses the fact that a walker found at site x at time t after making at least one step must have made his first jump from $x_0 = 0$ to x' at some time t' and subsequently found his way to site x in remaining time $t - t'$, as shown in Figure 5.1.

If the initial state of the walker is given by an initial distribution $p(x, 0) = p_0(x)$, we can write the probability of being in state x at time t as

$$p(x,t) = \int P(x-y,t)p_0(y)dy.$$

As shown in the Appendix, the evolution equation for $p(x, t)$ then can be derived directly from the equation (5.2). The type of the resulting equations depends on the choice of the waiting time distribution. When the waiting times are distributed exponentially, i.e. $w(t) = re^{-rt}$, (5.2) reduces to a regular integro-differential equation with jump kernel:

$$\frac{\partial}{\partial t}p(x,t) = r\int_{-\infty}^{\infty}[p(x-x',t) - p(x,t)]\mu(x')dx'. \tag{5.3}$$

For all other choices of the waiting times, the differential equation is history-dependent and does not represent a Markov process. For a particular choice of waiting times $w(t) = t^{-1-\beta}$, for instance, (5.2) is a fractional integro-differential equation

$$\frac{\partial^\beta}{\partial t^\beta}p(x,t) = \int_{-\infty}^{\infty}[p(x-x',t) - p(x,t)]\mu(x')dx'. \tag{5.4}$$

where we employ the so-called Caputo fractional derivative definition

$$\frac{d^\beta}{dt^\beta}f(t) = \frac{1}{\Gamma(1-\beta)}\int_0^t \frac{f'(\tau)}{(t-\tau)^\beta}d\tau. \tag{5.5}$$

Leaving further technical details to the Appendix, we would like to determine whether our model falls within the scope of this theory.

5.2. Numerical experiments based on fractional approach. While the dependence of the waiting times distribution on the step number does not correspond to the standard fractional dynamics, in Section 4.2 we have seen the evidence that, at the intermediate stage, the evolution may indeed be fractional with the empirical value of $\beta = 0.3$. Here we will provide further numerical justification that this is

indeed the case by showing that at the intermediate stage the time dependence of the joint distribution of grain boundary lengths and velocities can be described by a fractional PDE.

Suppose that the state of the grain boundary is described by a pair (v, l), where $l > 0$ and $v \in \mathbf{R}$ and that the distribution of (v, l) is given by $p(v, l, t)$. Further, suppose that the grain boundary velocity jump process satisfies the assumptions made in the previous section. We need to modify the equation (5.4) to take into account that, in addition to the velocity, a grain boundary is described by its length which changes continuously through disappearance events. The dependence on length can be incorporated into the equation (5.4) through a convective term that takes into account the relationship between the velocity and the length of the given interval.

In other words, we wish to consider the evolution of the joint density $p(v, l, t)$ described by the fractional integro-differential equation with a drift:

$$\frac{\partial^\beta}{\partial t^\beta} p(v, l, t) = v \frac{\partial}{\partial l} p(v, l, t) + \int_{-\infty}^{\infty} [p(v - v', l, t) - p(v, l, t)] \mu(v') dv', \tag{5.6}$$

where $\partial^\beta / \partial t$ stands for the Caputo fractional derivative, as given in equation (5.5) above, while $\partial / \partial l$ is the regular partial derivative with respect to the length variable.

Numerically, this equation is best solved by using Grunwald-Letnikov approximation of fractional derivative (see [21]):

$$\frac{\partial^\beta f(t)}{\partial t^\beta} = \lim_{h \to 0} \frac{1}{h^\beta} \sum_{k=0}^{[t/h]} \omega_k^{(\beta)} f(t - kh), \quad \text{where} \quad \omega_k^{(\beta)} = (-1)^k \left(\begin{array}{c} \beta \\ k \end{array} \right).$$

Taking $\beta = 0.3$ to conform with earlier observations, numerical solution of (5.6) can be obtained by using the explicit forward time centered space difference scheme, with $p_{i,j}^m$ representing the value of the discretized probability density after m steps, with velocity v in j-th bin and length l in i-th bin, i.e. $v \in [v_j, v_j + \Delta v], j = 1, \ldots, N_j$ and $l \in [l_i, l_i + \Delta l], i = 1, \ldots, N_i$, as follows:

$$p_{i,j}^{(m+1)} = p_{i,j}^{(m)} + \sum_{k=0}^{m} \omega_k^{(\beta)} [D_\beta v_j \Delta_l p_{i,j}^{(m-k)} + S_\beta I_{i,j}^{(m-k)}], \tag{5.7}$$

where the constants take the form $S_\beta = \dfrac{(\Delta t)^\beta}{(\Delta v)}$, $D_\beta = \dfrac{(\Delta t)^\beta}{(\Delta l)}$. The first derivative in l is computed using an upwind scheme

$$\Delta_l p_{i,j}^{(m-k)} = \left\{ \begin{array}{ll} p_{i,j}^{(m-k)} - p_{i-1,j}^{(m-k)}, & v_j \geq 0 \\ p_{i+1,j}^{(m-k)} - p_{i,j}^{(m-k)}, & v_j < 0 \end{array} \right.$$

where a natural boundary condition is assumed for the part of the domain with $v > 0$. The contribution of the jump part corresponds to the following discretization of the integral:

$$I_{i,j}^{(m-k)} = \sum_{s_l : j + s_l \in [1, N_j]} \mu_l [p_{i,j+s_l}^{(m-k)} - p_{i,j}^{(m-k)}], \tag{5.8}$$

where $\mu_l = \mu(x_l)$.

In the absence of the drift term and with purely diffusive jumps, this numerical scheme has been shown in [24] to be conditionally stable. While similar conjectures have been made in some more general cases, full analysis of stability and accuracy issues for the schemes involving fractional derivatives and jump kernels of this type are subject to further investigation and will be presented in subsequent works. Notice that fractional derivative in time introduces dependence on the past history, which brings in extra memory requirements for the corresponding numerical scheme. Luckily, weights ω decay almost exponentially as shown in Figure 5.2(a).

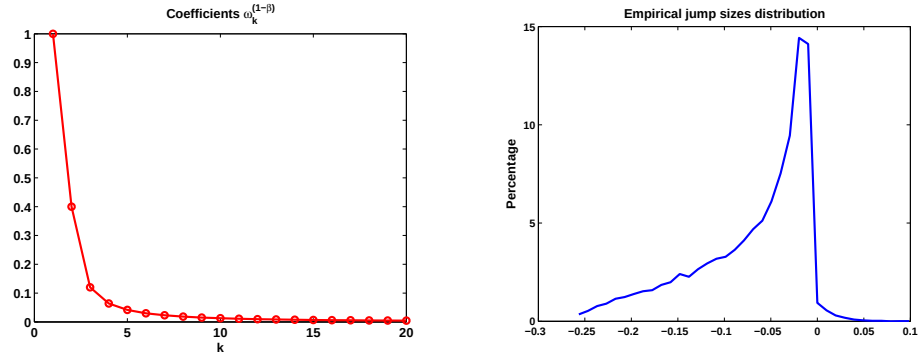

FIG. 5.2. *(a) Weights $\omega_k^{(\beta)}$ in Grunwald-Letnikov approximation of the fractional derivative, (b) Empirical jump sizes distribution $\mu = \{\mu_l\}$ used in the discretization of the jump integral (5.8).*

Similar to the previous section, we look at the evolution of 5000 grain boundaries for $f(x) = (x - 0.5)^2$. We determine $\mu(s)$ from the empirical jump probability density shown in Figure 5.2(b) constructed using data harvested from the deterministic simulation. We use μ to form the expression for the jump integral (5.8) and proceed by running the computational model (**??**) with $\beta = 0.3$ as in Figure 4.2. Figure 5.3 shows that the results of the the FPDE simulation (right) are in reasonable agreement with simulation (left) in the stable regime between 3000 and 4000 simulation steps. Both distributions narrow down with time and preserve singularity at the maximum, contrary to regular diffusive behavior. The dashed curve denotes the starting distribution, while the final shape is represented by the boldface curve.

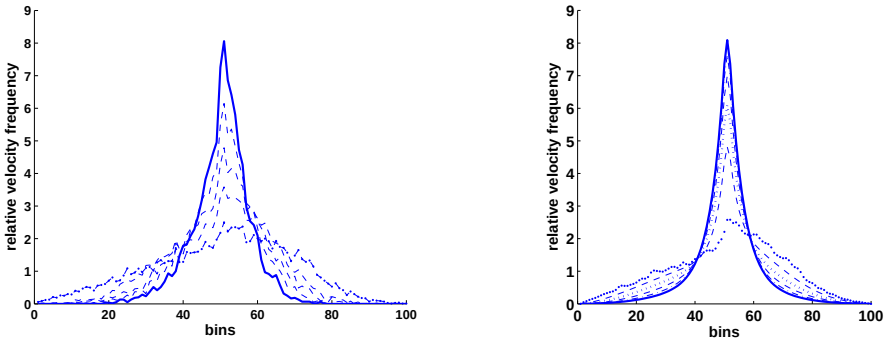

FIG. 5.3. *(a) Evolution of grain boundary velocities as collected from simulation; (b) numerical solution of the fractional equation (5.7). Snapshots are taken after every 200 steps, starting at 3000th step, with the shape after 4000 steps depicted with boldface font.*

Having made these observations, it becomes clear that the jump process underlying the grain growth dynamics in the simplified system is far from trivial. It is not just the fact that it does not fit into the regular diffusion framework, but also that due to the decaying disappearance rates, it deviates from the more general framework of continuous time random walks, which makes the analysis more complicated. By means of the generalized renewal theory, we have been able to completely determine the disappearance rates throughout the model evolution. Moreover, we have shown that the model bears striking similarity to the fractional sub-diffusion in an intermediate regime where most relevant distributions stabilize resulting in simpler evolution equation. While we have been able to successfully simulate both equations numerically, many interesting questions remain about the stability and accuracy of these implementations.

This kind of analysis readily suggests several directions of research in the context of medium-to-large scale 2d and 3d models that are currently under investigation. If we treat the effect of disappearance events on grain boundary distributions as that of a jump process, then which of the characteristics will be preserved when we go to higher space dimensions? As long as the waiting times and the magnitudes of jumps for the relevant quantities can be estimated, we can perform an in-depth analysis employing the tools derived above and use the results for validation and prediction of materials properties.

6. Discussion. One of the principal coarsening mechanisms of microstructural evolution is the motion of the triple junctions. The effect of topological changes (facet interchanges and disappearances) on this process is not yet understood. We propose a framework capable of describing the jump process associated with these events via a generalized continuous time random walk theory. We consider a reduced gradient flow model that neglects the curvature kinetic effects but retains other main characteristics of the evolution of triple junctions. We analyze the grain boundary distributions generated by the simplified dynamics. We show that the model possesses stable statistics for lengths, velocities and misorientations and demonstrate a subdiffusive nature of the evolution of grain boundary velocities. We show that the waiting times between the disappearance events are not identically distributed, but rather have exponential distributions that decay with time. This is one manifestation of the slowdown associated with coarsening. We identify the generalized renewal equation for the disappearance rates and confirm its validity via a comparison with simulations. We show that there is an intermediate regime within the simulation that can be described within the framework of the theory of continuous time random walks. We obtain a fractional evolution equation for a distribution of the grain boundary velocities and orientations that shows good agreement with the statistics generated by the gradient flow dynamics in the simplified model.

Although the results presented here are confined to the one-dimensional topology, we believe that the main attributes of the system behavior have been identified. We conjecture that the form of the fractional evolution equation should be preserved in higher dimensions. Numerical implementation and testing of the higher-dimensional model will be presented in future publications.

7. Acknowledgment. The authors wish to thank their colleagues Eva Eggeling, Gregory Rohrer and Anthony Rollett. Research supported by grants DMS 0405343 and DMR 0520425. DG acknowledges the support of DMS 0407361 and DK acknowledges the support of DMS 0305794. KB thanks S. Roberts and T. Shyu for their assistance.

8. Appendix. Evolution equations for Markov and non-Markov jump processes. Here we present a short derivation of the generalized master equation that produces equations (5.3) and (5.4) used in Section 5.1. Let us start with equation (5.2) and suppose as before that the initial state of the walker is given by an initial distribution $p(x,0) = p_0(x)$. In this situation, we can write the probability of being in state x at time t as

$$p(x,t) = \int P(x-y,t)p_0(y)dy \tag{8.1}$$

which yields a more general form of the random walk equation 5.2:

$$p(x,t) = p_0(x)\psi(t) + \int_0^t \int_{-\infty}^{\infty} p(x-x',t-t')\mu(x')w(t')dx'dt'. \tag{8.2}$$

We will now see that both equations (5.3) and (5.4) are simple consequences of the above equation for some special choices of parameters. For this purpose, it is convenient to work with equation (8.2) in Laplace space. Indeed, denote the Laplace time variable as u and the Laplace transforms of $p(x,t)$ and $w(t)$ by $\hat{p}(x,u)$ and $\hat{w}(u)$, respectively. Then we arrive at

$$\hat{p}(x,u) = \frac{p_0(x)(1-\hat{w}(u))}{u} + \hat{w}(u)\int_{-\infty}^{\infty} \hat{p}(x-x',u)\mu(x')dx'. \tag{8.3}$$

We can look at this equation from a slightly different perspective, similar to that offered in [20]. After some simple algebra we can rewrite (8.3) as follows:

$$\frac{1-\hat{w}(u)}{u\hat{w}(u)}(u\hat{p}(x,u) - p_0(x)) + \hat{p}(x,u) = \int_{-\infty}^{\infty} \hat{p}(x-x',u)\mu(x')dx'$$

and let

$$\hat{\Phi}(u) = \frac{1-\hat{w}(u)}{u\hat{w}(u)}.$$

Then we have

$$\hat{\Phi}(u)(u\hat{p}(x,u) - p_0(x)) = \int_{-\infty}^{\infty} [\hat{p}(x-x',u) - \hat{p}(x,u)]\mu(x')dx', \tag{8.4}$$

and by taking inverse Laplace transform

$$\int_0^{\infty} \Phi(t-t')\frac{\partial}{\partial t}p(x,t')dt' = \int_{-\infty}^{\infty} [p(x-x',t) - p(x,t)]\mu(x')dx'. \tag{8.5}$$

Following [20] we call $\Phi(t)$ the "memory function" of the CTRW.

It is easy to see that (8.5) formally reduces to a differential equation if the process is Markov ("memoryless"). Then $\Phi(t) = \frac{1}{r}\delta(t)$, where $r = \text{const}$ and

$$\frac{\partial}{\partial t}p(x,t) = r\int_{-\infty}^{\infty} [p(x-x',t) - p(x,t)]\mu(x')dx'. \tag{8.6}$$

This is equivalent to having $\hat{\Phi}(u) = \frac{1}{r}$ and

$$\hat{w}(u) = \frac{r}{u+r} \text{ and } w(t) = re^{-rt}.$$

In other words, in order to have a Markovian CTRW one needs to have exponentially distributed waiting times. It is useful for us to derive a generalized master equation of the form (8.6) for a much wider class of processes. Namely, suppose

$$\hat{\Phi}(u) = u^{\beta-1}, \tag{8.7}$$

then equation (8.4) becomes

$$(u^{\beta}\hat{p}(x,u) - p_0(x)u^{\beta-1}) = \int_{-\infty}^{\infty} [p(x-x',t) - p(x,t)]\mu(x')dx', \tag{8.8}$$

which corresponds to

$$\frac{\partial^{\beta}}{\partial t^{\beta}} p(x,t) = \int_{-\infty}^{\infty} [p(x-x',t) - p(x,t)]\mu(x')dx'. \tag{8.9}$$

Here we employ the so-called Caputo fractional derivative definition

$$\frac{d^{\beta}}{dt^{\beta}} f(t) = \frac{1}{\Gamma(1-\beta)} \int_0^t \frac{f'(\tau)}{(t-\tau)^{\beta}} d\tau,$$

for which

$$\mathcal{L}\Big[\frac{d^{\beta}}{dt^{\beta}} f(t)\Big] = u^{\beta}\hat{f}(u) - u^{\beta-1}f(0).$$

The choice of $\hat{\Phi}(u)$ in (8.7) suggests the form of waiting times distribution that generalizes exponential behavior of the Markovian case. Namely,

$$\hat{w}(u) = \frac{1}{u^{\beta}+1},$$

which after inversion gives

$$w(t) = -\frac{d}{dt} E_{\beta}(-t^{\beta}), \tag{8.10}$$

where $E_{\beta} = \sum_{n=0}^{\infty} \frac{z^n}{\Gamma(\beta n + 1)}$ is the Mittag-Leffler function, which interpolates between the stretched exponential form and long-time inverse power law behavior [18]. This is the only choice of a waiting time distribution that allows one to transform the basic CTRW equation (8.2) directly into a fractional evolution equation without a limiting procedure (see [8]). As shown in [20], we get the following asymptotic behavior for the waiting times in this case:

$$\begin{aligned} w(t) &= \frac{1}{t^{1-\beta}} \sum_{n=0}^{\infty} (-1)^n \frac{t^{\beta n}}{\Gamma(\beta n + \beta)}, \quad t \geq 0, \\ w(t) &\sim \frac{\sin \beta n}{\pi} \frac{\Gamma(\beta+1)}{t^{\beta+1}}, \qquad\qquad t \to \infty. \end{aligned} \tag{8.11}$$

When $\beta = 1$ we recover the exponential waiting time behavior of the Markovian case. Also, note that this discussion applies to the generalized renewal equation (4.10) which can be converted to a fractional ODE. In the case of exponential waiting times with arbitrary jump sizes, equation (8.9) coincides with the evolution equation for the Poisson jump process as developed in the theory of Levy processes (see [2], [19]).

REFERENCES

[1] S. Agmon, A. Douglis, and L. Nirenberg. Estimates near the boundary for solutions of elliptic partial differential equations satisfying general boundary conditions, II. *Comm. Pure Appl. Math.*, 17:35–92, 1964.

[2] D. Applebaum, Levy Processes and Stochastic Calculus, Cambridge studies in advanced mathematics, 93, Cambridge, 2004.

[3] H.V. Atkinson, Theories on normal grain growth in pure single phase systems, Acta Metall., 36 (1988) 469–491.

[4] K. Barmak, M. Emelianenko, D. Golovaty, D. Kinderlehrer, and S. Ta'asan, A new perspective on texture evolution, to appear in *Int. J. of Num. Anal. and Model.*, 2008.

[5] L. Bronsard and F. Reitich, On three-phase boundary motion and the singular limit of a vector-valued Ginzburg-Landau equation. *Arch. Rat. Mech. Anal.*, 124:355–379, 1993

[6] E. Cinlar, Introduction to Stochastic Processes, Prentice Hall, 1997.

[7] D.R. Cox, Renewal theory, Methuen & Co., 1970.

[8] R. Gorenflo, A. Vivoli, F. Mainardi, "Discrete and Continuous Random Walk Models for Space-time Fractional Derivatives", J. Math. Sci., **vol. 132**, No. 5, 2006.

[9] E.A. Holm, G.N. Hassold, and M.A. Miodownik, Acta Mater., Vol. 49 (2001) 2981.

[10] B.D. Hughes, Random Walks and Random Environments, Volume I: Random Walks, Oxford University Press, 1995.

[11] D. Kinderlehrer, I. Livshits, G.S. Rohrer, S. Ta'asan, S. and P. Yu, "Mesoscale evolution of the grain boundary character distribution, Recrystallization and Grain Growth", Materials Science Forum vols 467-470, 1063-1068, 2004.

[12] D. Kinderlehrer, J. Lee, I. Livshits and S. Ta'asan. Mesoscale simulation of grain growth. In Raabe, D. et al., editors, *Continuum Scale Simulation of Engineering Materials*, pages 361–372, Wiley-VCH Verlag, Weinheim, 2004.

[13] D. Kinderlehrer, I. Livshits and S. Ta'asan, "A variational approach to modeling and simulation of grain growth", SIAM J. Sci. Comput. Vol. 28, No. 5, pp. 1694-1715, 2006.

[14] D. Kinderlehrer and C. Liu. Evolution of grain boundaries. *Math. Models and Meth. Appl. Math.*, 11.4:713–729, 2001.

[15] P. Mellars, "Going East: New Genetic and Archaeological Perspectives on the Modern Human Colonization of Eurasia", Science, 313, 796 - 800, 2006.

[16] W. W. Mullins. Two-dimensional motion of idealized grain boundaries. *J. Appl. Phys.*, 27:900–904, 1956.

[17] W. W. Mullins. Solid surface morphologies governed by capillarity. *Metal Surfaces: Structure, Energetics, and Kinetics*, ASM, Cleveland, 17–66, 1963.

[18] R. Metzler, J. Klafter, The Random Walk's Guide to Anomalous Diffusion: A Fractional Dynamics Approach, Physics Reports, 339

[19] M. Grigoriu, Stochastic Calculus, Applications in Science and Engineering, Birkhauser, Boston, 2002.

[20] F. Mainardi et al, Fractional calculus and continuous-time finance II: the waiting-time distribution, Physica A, 287, p.468-481, 2000.

[21] I. Podlubny, Fractional Differential Equations, Academic Press, 1999

[22] M. Upmanyu, G.N. Hassold, A. Kazaryan, E.A. Holm, Y. Wang, B. Patton, D.J. Srolovitz, Interface Science, Vol. 10 (2002) 201.

[23] G.H. Weiss, Aspects and Applications of the Random Walk, North Holland Press, Amsterdam, 1994.

[24] S.B. Yuste, L. Acedo, "An explicit finite difference method and a new Von Neumann-type stability analysis for fractional diffusion equation", SIAM J. Numer. Anal., Vol.42, No.5, p. 1862-1974, 2005.

[25] G. Zaslavsky, Hamiltonian Chaos and Fractional Dynamics, Oxford University Press, Oxford, 2005.